Modelling of magnetron sputtering process

T. Kubart, R. Novák

Department of Physics, Faculty of Mechanical Engineering,
Technická 4, CTU Prague, 160 07, Czech Republic
Tomas.Kubart@fs.cvut.cz

J. Valter

HVM Plasma, spol. s r. o.,
Na Hutmance 2, 158 00, Prague 5, Czech Republic

Received 17 May 2004

Magnetron sputtering is a technique commonly used in modern industry for thin films deposition with an accurate control of the coating parameters. In the magnetron sputtering system the target material is sputtered off by plasma ions. The plasma is sustained by an electrical discharge and magnetically confined in the target vicinity. This results in much higher sputtering rate, lower operating pressure and lower discharge voltage compared to a glow discharge diode sputtering systems. The modelling of magnetron sputtering is essential for the design of new coating systems. It enables efficient, low-cost and time-saving optimisation of the system. In this paper information on modelling of magnetrons at the Department of physics, Faculty of Mechanical Engineering CTU is given. Our work consists of two parts. The magnetic field of a given magnet array is first modelled by the finite element method and the computed field is then used for simulation of the erosion process by a Monte-Carlo model. The results are compared with measured erosion tracks and the accuracy of the model is discussed.

PACS: 52.77.Dq, 81.15.Jj
Key words: magnetron sputtering, plasma modelling

1 Introduction

DC planar magnetron sputtering is widely used for the deposition of metallic thin films. When the sputtering is carried out in a mixture of working gas (Ar) with reactive gas (O_2, N_2, CH_x) the range of possible coatings is very wide, including e.g. ceramic insulating layers, hard nitride and carbide based coatings, semiconductors and many others. Taking advantage of the magnetic field, a magnetron operates at much higher power density, lower pressure and lower discharge voltage compared to the simple diode sputtering. The applied magnetic field confines energetic electrons near the cathode creating thus a dense plasma just above the target surface. The target material atoms are then efficiently sputtered off by the ion impingement, diffuse through the working gas and condense on the coated surface where they possibly react with the reactive gas.

Compact coating with bulk material properties may be prepared with sufficient bombardment of growing surface by the working gas ions. This can be achieved with an additional magnetic field that deviate the trajectories of some energetic

electrons from the glow region towards the substrate (unbalanced magnetron [1]). Magnetron system has the advantage of high deposition rate and very good versatility. Moreover, coating systems with virtually no size limitations can be designed for large area coatings [2]. One of the important issues of the magnetron sputtering is related to the target erosion. Its possible nonuniformity decreases the target utilization several times and variations in the deposited layer thickness and composition may appear. The computer simulation of the sputtering rate distribution is used to prevent these harmful effects. Other models deal with the transport, chemical reactions and the film growth providing more control over the whole process.

Magnetron discharge is a kind of low pressure glow discharge. The plasma density is relatively low with the degree of ionization about 10^{-4} and the created electrons do not undergo many collisions so they are not in equilibrium. Therefore, the discharge has to be modelled by particle simulations [3]. Typical magnetron operates at the pressure range $0.1 \div 1$ Pa, discharge voltage 500 V, parallel magnetic field 0.03 T, and the current density 20 mA cm^{-2}. Self–consistent particle–in–cell (PIC) models completed with Monte–Carlo (MC) collisions are a suitable approach giving full information about the process [4], but it requires a very long calculation time. To reduce computation costs the more simple method proposed in [5] was used. Only the secondary electrons are traced and their collisions are simulated by MC. The electric and magnetic fields are considered to be unaffected by the plasma. The target erosion is determined from the ion impact density assuming constant sputtering yield.

It is known from optical emission measurements [6] that almost all applied voltage drop linearly in the sheath layer. The sheath thickness s for a plane diode is given by the Child–Langmuir law

$$j_c = \frac{4\varepsilon_0}{9}\sqrt{\frac{2e}{M}}\frac{V_0^{3/2}}{s^2}$$

where j_c is the current density for a voltage V_0, e the elementary charge, and M the ion mass. However, only a scaling law considering magnetic field exists [6]

$$s = C\frac{V^{7/8}}{I^{1/2}B_0^{1/4}}$$

where C is constant of aparatus, I, V discharge current and voltage and B_0 the parallel field strength. The sheath thickness could be substitued with Larmor radius of corresponding electron [7].

Magnetic field may be solved by wide range of different methods. When the magnetic system is composed only of permanent magnets with constant magnetization, the magnetostatic approach could be [8]. In such case the magnetic regions are replaced with surface magnetic charges and magnetic flux density is obtained by an analogy with the electrostatics. Magnetic field of current carrying regions (coils) can be superimposed using the Biot–Savart law. This method is simple and gives an analytical expression but doesn't allow to compute systems with ferromagnetic parts like pole pieces or targets often present in industrial magnetron sputtering

devices. Therefore a more general method has to be used. The most common one is the finite element method (FEM) which solves complex geometry with nonlinear materials. Thus we used a FEM results as an input for the erosion simulation code.

2 Model

A rectangular planar magnetron was studied. Computed magnetic system is shown in Fig. 1a and Fig. 1b where the transverse cross–section is depicted. We used this cross–section for more simple 2–D model and considered the magnetron as very long. The coordinate system is situated with y axis perpendicular to the target surface, x is pointed transverse and z along the target. Magnetic system consists of permanent magnets and iron back plate with pole pieces.

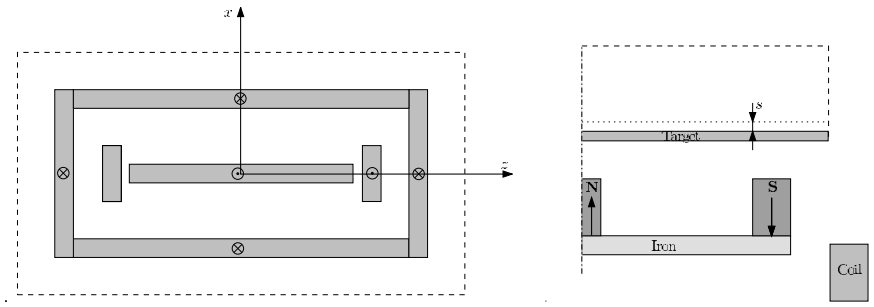

(a) (b)

Fig. 1. (a) Top view of a rectangular magnetron magnetic system. (b) Two-dimensional model based on a cross-section in x axe of the (a). Boundaries of computed domain are marked with dashed lines.

2.1 Electric and magnetic field

The electric field was assumed to be unaffected by the plasma and constant over the whole target surface. The field intensity in the sheath layer corresponds to full voltage V applied to the target while in the plasma volume it is supposed to be zero. The thickness of the sheath s is considered equal to the Larmor radius of an electron of energy V in magnetic field B_0. Magnetic field was solved using FEM software Ansys version 5.7. 2–D cross–section was calculated using scalar vector potential approach and 3–D model with reduced scalar potential. To reduce computation time, symmetries of the problem were utilized. Therefore in the 2–D case only one half of the cross–section was calculated while in 3–D only the first quadrant was solved and the complete field was obtained by mirroring. The boundary condition on the free surfaces was satisfied by infinite elements, considering the decay of the field to zero far from the magnets.

2.2 Equation of motion

Equation of motion of a charged particle in $\mathbf{E} \times \mathbf{B}$ field

$$\frac{d^2\mathbf{x}}{dt^2} = \frac{q}{m}\left(\mathbf{E} + \frac{d\mathbf{x}}{dt} \times \mathbf{B}\right)$$

can be solved by different numerical schemes [9]. We used the fourth–order Runge–Kutta method because of its high accuracy. The Leap–Frog integrator is faster, however in case of long mean free path shorter time step is required and it is impossible to use variable time step. In our model time step in bulk plasma was 50 times longer then in sheath layer in order to avoid numerical heating of electrons in a strong electric field. An electron is traced until its energy decreases below the ionization potential of argon or moves away of the calculation domain. First electron is created in a fixed point and then the emission point is selected randomly according to the ion impingement density on the target surface. New electrons are created at the end of the sheath (dotted line in Fig. 1.b) with energy V_0.

2.3 Collision

It is tested after each time step if an collision occurs. Only elastic, excitation and single ionization collisions are taken into account. The collision probability is proportional to the sum of the total cross–sections for each collision type. When a collision occurs, its type is distinguished following individual cross-sections. The energy of electron is decreased by 11.55 eV after excitation, by 15.76 eV after ionization and by 0.3 eV after elastic collision. Since the angular distribution of electrons scattered in argon is similar for all three collisions [10], the velocity direction after collision is determined according to the differential cross-section of elastic scattering [11]. Trajectories of created ions are affected very little by magnetic field due to their high mass so they were assumed to be unmagnetized. Also collisions of ions with neutral gas were neglected ($\lambda_i \approx 20$ mm at 0.5 Pa). Therefore the ions created in collisions fell directly to the target without any transverse motion.

2.4 Recapture of secondary electrons

In the MC simulations of the magnetron sputtering, the energy of created secondary electrons (SE) is predominantly assumed to be zero. Real SE have the average energy about 4 eV and a cosine distribution of the initial velocity direction [12]. Particles with nonzero value of this velocity can reached the target surface during their movement back (turned by $\mathbf{B}$) and be captured there. It results in a decrease of the effective SE yield γ_{eff} compared to the values obtained by ion beam measurements γ_{se} [13]. A model is described in [14] for the numerical studies of SE recapture effects in a simple configuration. The obtained results confirmed the previous estimate $\gamma_{\mathrm{eff}} = \frac{1}{2}\gamma_{\mathrm{se}}$, however, the fraction of recaptured electrons were dependent on the position of emission. As a consequence, the erosion rate distribution may be affected by this effect. Our aim was to examine the influence of the SE

recapture on the shape of the erosion track under real condition. In order to study the SE recapture, simulations with different values of the initial SE energy E_0 were performed. The electrons were emitted from the target surface with cosine angular distribution.

3 Results and discussion

Simulations were performed for the argon pressure 0.5 Pa, discharge voltage $V_0 = 500$ V, and sheath thickness $s = 3$ mm. The time step was chosen to be

$$\Delta t = 1 \times 10^{-12} \text{ s},$$

based on the observation of total energy of particles in sheath. In the bulk plasma ($y > y_{\text{target}} + 2 \times s$) the time step was 50 times longer then in sheath layer. The number of emitted electrons was 1 000 for 2–D simulation and 20 000 for 3–D. 2–D results are shown for several coil currents I_c, while presented 3–D results were obtained without the additional coil.

3.1 2–D

Magnetic flux density components on the target surface for two value of the coil current are shown in Fig. 2. The maximum erosion lies under the point where the

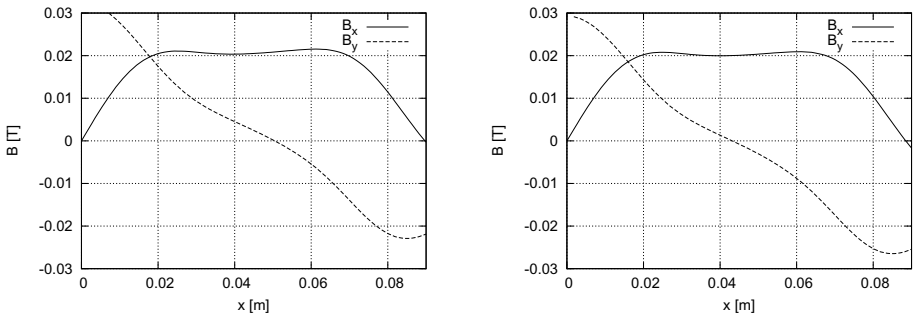

(a) $I_c = 0$ A (b) $I_c = 3$ A

Fig. 2. Components of magnetic field on the target surface.

flux density is parallel to the target ($B_y = 0$) as expected. The position of this point is influenced by the coil current so all the erosion track moves accordingly. Field lines of the magnetic field (Fig. 3) document the transition from balanced ($I_c = 0$) to unbalanced ($I_c = 3$) magnetron. Distribution of the ionization points plotted on these figures corresponds to the depicted field lines. In case of the unbalanced magnetron some electrons escape along the open field lines and create a plasma in the substrate region (left top corner). It increases many times the ion bombardment of the growing layer. Then the model gives also an information about the substrate conditions.

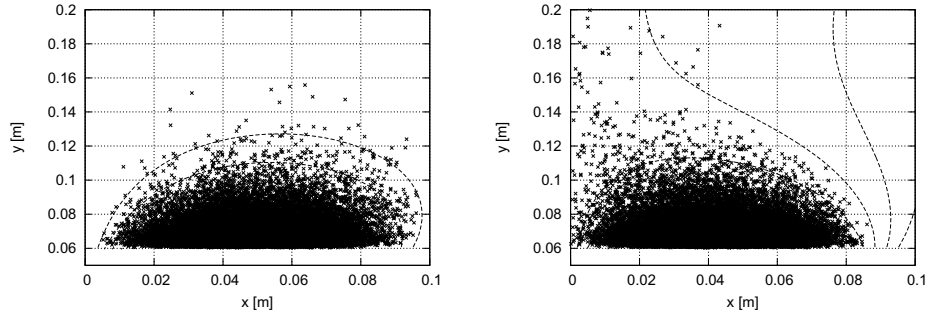

(a) $I_c = 0$ A (b) $I_c = 3$ A

Fig. 3. Ionization points and magnetic field lines for two coil currents.

The erosion profiles for different coil currents are shown in Fig. 4. All graphs are normalized to the maximum value. When compared to the Fig. 2 it can be recognized the significance of the point $B_y = 0$. The maximum of the erosion moves with increasing coil current towards the target center which can be used for higher target utilization. However, as is shown in Fig. 3, the coil current can not be selected independently since its influence on plasma distribution.

The accuracy of the model was verified by comparison with measurement of target eroded at $I_c = 1.5$A (Fig. 5). Both curves agree well. There are some differences mainly at the margins which probably result from the redeposition of backscattered particles. The influence of redeposition could be readily recognized in the centre of the target ($x = 0$), where a negative erosion rate was measured which means a layer had grown there. Therefore the accuracy of our model could be increased the most by a tracing of the sputtered particles.

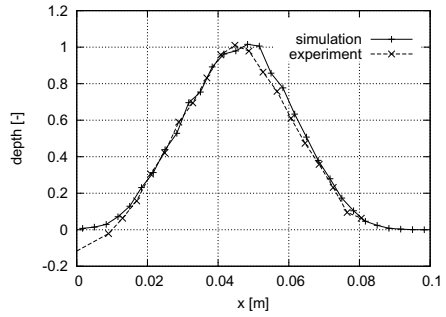

Fig. 4. The erosion profiles measured and obtained by simulation at I_c=1.5 A.

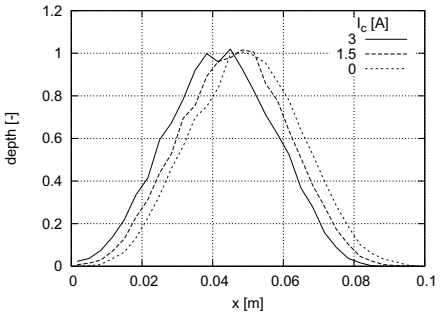

Fig. 5. The calculated erosion profiles for different coil currents

The influence of the SE recapture was tested for two values of $E_0 = 0$ and 4 eV. Computed results are shown in Fig. 6 for the coil current 3 A. Although 51% of SE emitted with $E_0 = 4$ eV were recaptured, there is no difference in the shape of the

erosion rate profiles. The lines for $E_0 = 0$ eV is smoother due to higher number of ionizations because the number of emitted electrons was fixed. As a result of our simulation we can say that for the modelling of the erosion it is possible to neglect the SE recapture. The only apparent result caused by this effect is an increase of the discharge voltage described by the introduction of. Models with zero initial energy are more efficient because electrons may be emitted from the sheath edge and there is no lost of electrons by recapture.

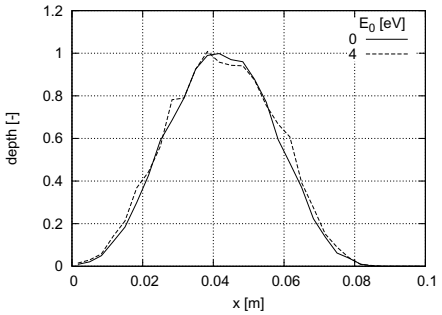

Fig. 6. The erosion profiles calculated for two values of initial secondary electron energy E_0. Both simulation were performed for $I = 3$ A.

3.2 3–D

Only simulations without coil are presented for the full magnetron. In Fig. 7 the contour lines of the parallel component of the magnetic flux density B_p are plotted. In the same figure the line where $B_y = 0$ is plotted (thick solid line) in order to give information about the field line tunnel shape. Note the shape of this line for later comparison with simulation results.

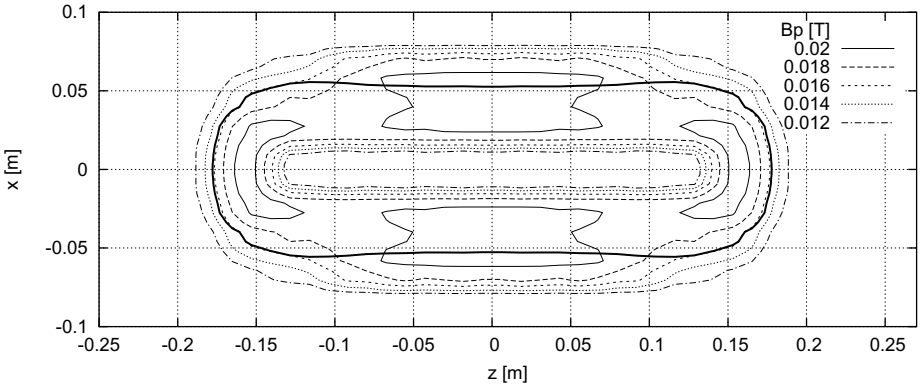

Fig. 7. Contours of calculated parallel flux density B_p on the target surface. The line of $B_y = 0$ is plotted with thick solid line.

Distribution of ionization points is shown in Fig. 8 and Fig. 9 shows the contour lines of normalized values of ion densities. The most interesting result is clear asymmetry in the erosion depth in spite of the symmetry of the magnetic field as shown in Fig. 7. $\mathbf{E}\times\mathbf{B}$ drift motion of electrons is clockwise, hence the erosion rate is the highest at the end (outlet) of the bend. The asymmetry is most probably caused by gradients of magnetic field in the bend.

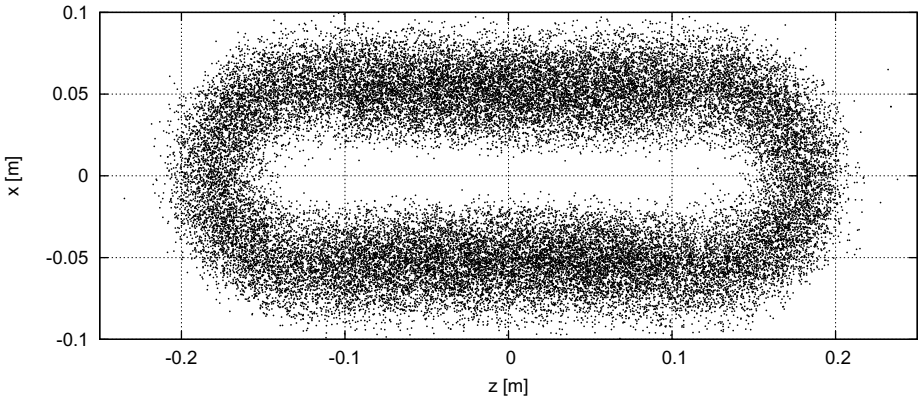

Fig. 8. The ionization points obtained by simulation at zero coil current.

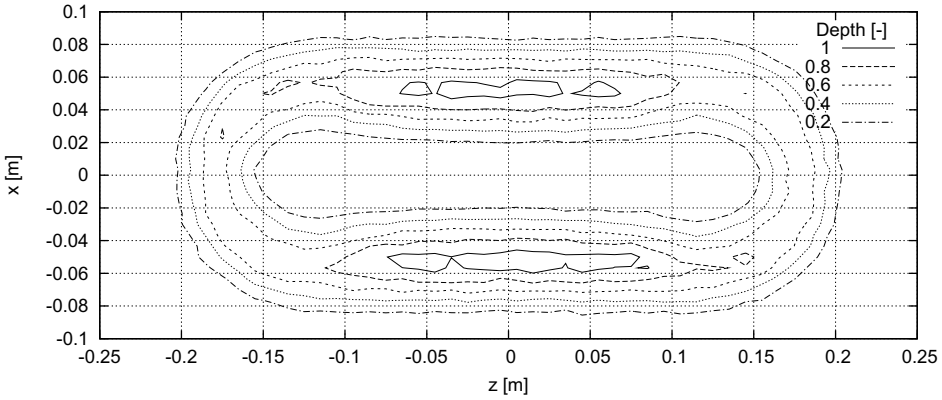

Fig. 9. The erosion of the target corresponding to previous picture.
The depth is normalized.

4 Conclusions

We prepared a collisional model of magnetron discharge for simulation of the target erosion. Using the model simulations of erosion were performed considering

the recapture of secondary electrons. It has been confirmed that this recapture has no influence on the target erosion distribution and results only in a decrease of the effective secondary electron yield. 3–D erosion model allows us to study processes in a real magnetic field configuration of rectangular magnetrons. Main result is the asymmetrical erosion in symmetrical magnetic field which results probably from the magnetic field gradients in the bend. Such effect may dramatically influence the local erosion rate and decrease the target yield a lot. Comparison of our simulation results with experimental data shows that the accuracy of our model can be increased the most by tracing of sputtered particles in order to take into account the redeposition of backscattered atoms.

References

[1] Window, B., Savvides, N.: J. Vac. Sci. Technol. **A4**(2) (1986) 196-202

[2] R. Kukla: Surface and Coatings Technology **93** (1997) 1–6.

[3] A. Bogaerts, R. Gijbels: Vacuum **69** (2003) 37–52.

[4] K. Nanbu, S. Kondo: *Jpn. J. Appl. Phys.* 36 (1997) 4808-4814.

[5] T. E. Sheridan, M. J. Goeckner, J.Goree: J. Vac. Sci. Technol. **A8**(1) (1990) 30–37.

[6] L. Gu, M. A. Lieberman: J. Vac. Sci. Technol. **A6**(5) (1988) 2960–2964.

[7] C. H. Shon, J. K. Lee, Y. Yang, T. H. Chung: IEEE Trans. on Plasma Sci. **26**(6) (1998) 1635–1644.

[8] R. P. Feynman, R. B. Leighton, M. Sands: *The Feynman lectures on Physics.* 2nd edition. Reading: Addison-Wesley, 1964.

[9] C. K. Birdsall: IEEE Trans. on Plasma Sci. **19**(2) (1991) 65–85.

[10] H. S. W. Massey, E. H. S. Burhop, H. B. Gilbody: *Electronic and Ionic Impact Phenomena,* 2nd edition. Oxford: Clarendon, 1969–1974.

[11] S. N. Nahar, J. M. Wadehra: Physical Rev. A. 35(5) (1987) 2051–2064.

[12] Chapman, B., *Glow Discharge Processes,* New York: Willey, 1980.

[13] M. A. Lieberman, A. J. Lichtenberg: *Principles of Plasma Discharges and Materials Processing*, New York: Willey, 1994.

[14] G. Buyle: *Vacuum.* 70 (2003) 29–35.